International Journal of Recent Technology and Engineering (IJRTE)
ISSN: 2277-3878 (Online), Volume-8 Issue-2, July 2019

Scaling of Turbulent Spectra Measured in Mobile Bed Flows and Estimation of Turbulent Kinetic Energy Budgets

Ratul Das

Abstract*: This study aims at quantifying experimentally the influence of bed load transport on velocity power spectrum of acoustic Doppler Velocimeter (ADV) and turbulent kinetic energy budget. Hydraulic flume was used for experimental investigations for bed load transport. Uniform size of gravels (d_{50} = 4 mm) were injected into the flows without bed-forms development and compared with those in clear water flows. A 5 cm down looking Vectrino$^+$ of 10 MHz acoustic frequency was used to measure the velocity of flows. The velocity signals produced spikes in the Vectrino$^+$ data on account of instrument noise and high-frequency fluctuations. Therefore, de-spiking and removal of contaminated data were very much essential to obtain clear velocity power spectra for the ADV data sets. The velocity power spectra of filtered dataset followed the Kolmogorov "–5/3 scaling-law" in the inertial frequency range. At low frequencies, another scaling regime with spectral slope of about −1.0 is found resulting a shifting of turbulent power production subrange towards the high frequency regime and it is interpreted as the signature of sediment mobility without bed form development. Interestingly, the bed lad transport reduced the TKE dissipation rate and sharply changed the pressure energy diffusion rate which corroborated a gain in turbulence production.

Index Terms*: Bed-load, bed-forms, clear-water flows, energy dissipation, mobile-bed, velocity power spectra.

I. INTRODUCTION

In mobile bed hydraulics the sediment interactions with the flowing fluid and channel bed corroborate the exchange of particle momentum in terms of turbulent kinetic energy flux. Significant attempts have been made since few decades in this regard: yet, the origin and exploration of total energy flux and turbulent production level during bed load transport are still challenging [1-6]. Advancement of flow measuring instruments and data processing methodologies puts new impetus to explore this. Velocity power spectrum of acoustic Doppler velocimetry (ADV) time series is most significant to represents different spectral sub-regimes. In general, the time series measured by ADV contain furious spikes which produce an unrealistic spectral scaling regime [7]. These spikes appear on account of Doppler noise, fluctuations and configurations of ADV probe used for recording the velocity signals [7-13]. Therefore, handling of such ADV time series needs utmost care to obtain three dimensional velocity field and other turbulence characteristics. Since past few years many authors presented the filtration process of ADV velocity signals fitting with the inertial sub range of a velocity power spectrum but the computation approach still remained challenging. The method developed by Goring and Nikora, [9] can efficiently detect and remove spikes from ADV time series. Recently, Dey and Das, [14]; Dey et al. [15] applied this acceleration thresholding method for decontamination of ADV velocity signals in rough bed and mobile sand bed, respectively. A smart filtration technique requires some additional steps of reconstructing velocity signals at the locations of spurious spikes [9]. Many researchers [16-21] have studied extensively the power spectral densities in wall-bounded turbulent flows to delineate the inertial sub range of velocity power spectrum. In general, a velocity power spectrum consists of three scaling sub ranges. The scaling sub range at low frequencies is often referred to production sub range and characterized by a −1 spectral slope [20, 22] following a spectral regime with −5/3 spectral slope at intermediate frequencies called inertial sub range [23]. The third scaling sub range is known as viscous sub range where spectral density decays much faster than the inertial sub range [24, 25]. Fig.1 represents a schematic of three scaling regimes in a velocity power spectrum.

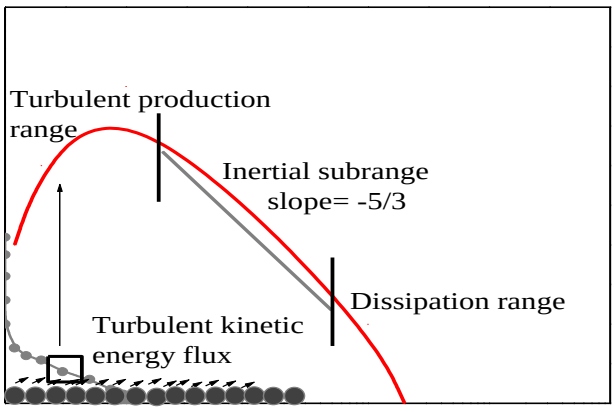

Fig.1 schematic of scaling regimes in a velocity power spectrum

Revised Manuscript Received on 30 July 2019.
***** Correspondence Author
Ratul Das*, Civil Engineering Department, National Institute of Technology Agartala, Tripura.

The frequency range of these sub regimes represents the geomorphological characteristics of channel bed and many issues of mobile bed hydraulics. Moreover, considerable attempts are made to investigate the influence of bed load transport on overlying flows.

Nikora and Goring [25] observed the differences in energy dissipation over a weakly mobile-beds and immobile-beds and further recommended [26] an additional range for refinement of spectrum that consisted four ranges of scales with different spectral behavior. Some experimental studies revealed a near-bed momentum deficit and reduction of stream wise velocity due to collisions of bed-particles during bed load transport [27- 29]. Many researchers [30- 36] observed that the bed load transport are influenced by the transient coherent flow structures and the size of these turbulent flow structures are found to the scale with flow depth. In some other studies, it is noted that the individual bed particles or clusters of particles offers frictional force and influences the near bed flow [3, 5, 24, 34, 37-42]. In this paper, we attempt to address the influence of bed load transport on spectral sub regimes and TKE-budget under two flow conditions: (1) bed load transport and (2) under clear water flows.

II. CONCEPTUAL FRAME WORK

The conventional practice followed to analyze the time series of velocity components in any direction (say u_i,) is to represent them with mean value, $\bar{u}_i$ and a fluctuating part, u_i':

$$u_i = \bar{u}_i + u_i' \tag{1}$$

Fig.2a represents a velocity power spectra (S_{uu}, S_{vv} and S_{ww}) recorded from the ADV. Here, we illustrate one example of three dimensional flow field (u, v and w) from ADV data sets. These data sets were chosen for illustrative purposes. As the temporal variations for the three time series that we analyses in this work show similar general behavior; we only plot one record (1.25 mm above the bed) for illustrative purpose. The data plots contain furious spikes and the procedure we follow to filter the data set is:

Firstly, we construct the power spectrum to identify the peaks of energy with a value higher than the 99% significance level (Fig.2a). Once identified, we have gone through an appropriate filtering process for removal of contaminated data form the time series. Secondly, we reconstruct the power spectrum from the filtered data and reiterate the procedure until all such signals are removed (Fig.2b). Therefore, filtered time series of velocity fluctuations in any direction need to be satisfied the Kolmogorov -5/3 scaling laws in the inertial frequency range of the velocity power spectrum, S_{uu} expressed as [43]:

$$S_{uu}(k_w) = C\,\varepsilon^{\frac{2}{3}} k_w^{\frac{-5}{3}} \tag{2}$$

where, k_w = radian wave number in streamwise direction, $S_{uu}(k_w)$ = wavenumber spectrum for u', ε = the rate of TKE dissipation and C = constant approximately equal to 0.5 [44].

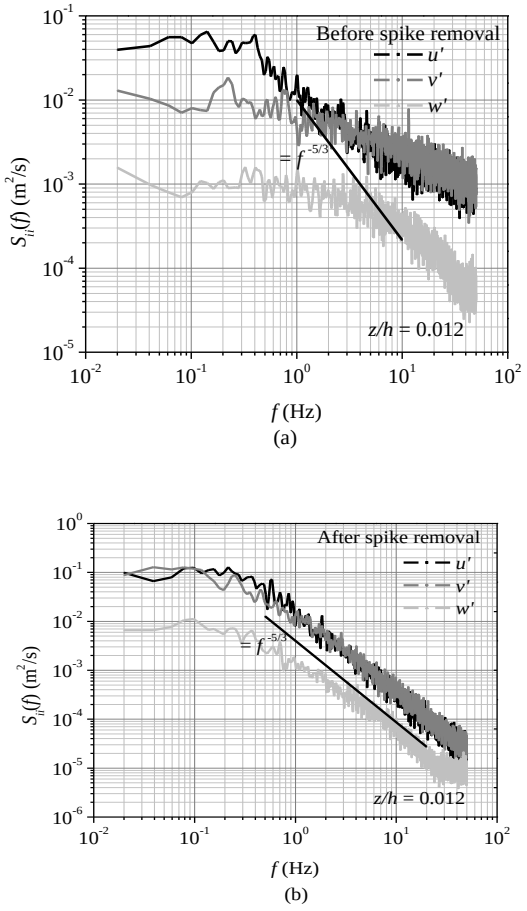

Fig. 2 velocity power spectra (a) before filtration of data (b) after filtration of data

Spectral density constructed from filtered ADV velocity signals are used to obtain the rate of TKE dissipation using Eq.(2), as:

$$\varepsilon = \left(\frac{S_{uu}(k_w) k_w^{1.66}}{C} \right)^{1.5} \tag{3}$$

Finally, the TKE-budget analysis is performed with the hypothesis of Nezu and Nakagawa [24] for uniform flows, given as:

$$\overbrace{-\overline{u'w'}\frac{\partial \bar{u}}{\partial z}}^{TKE-production} = \overbrace{\frac{\partial \overline{f_k}}{\partial z}}^{TKE-diffusion} + \overbrace{\frac{1}{\rho}\cdot\frac{\partial}{\partial z}(\overline{p'w'})}^{Pressure-diffusion} - \overbrace{\upsilon\frac{\partial^2 \overline{k}}{\partial z^2}}^{Viscous-diffusion} + \varepsilon \tag{4}$$

where, u' = stream wise velocity fluctuations, w' = velocity fluctuations in vertical direction, p' = fluctuations of time-averaged pressure intensity and k = term associated to turbulent energy. In Eq.(4) the viscous diffusion part is not significant in case of large flow Reynolds numbers. All the terms in Eq. (4) are determined experimentally except pressure diffusion rate.

III. EXPERIMENTAL PROCEDURE

A rectangular open-channel of 15 m long, 0.90 m wide and 0.80 m deep fitted with side glass wall was used to conduct the experiments. Fig. 3 shows the schematic of experimental set up for mobile bed flow experiments.

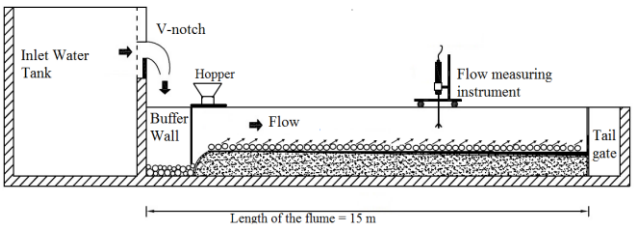

Fig. 3. Schematic of experimental set up

A calibrated V-notch weir was used to measure water discharge in the flume and the flow depth was regulated by a tail gate. The experimental programme consisted two runs: the first was over fixed bed under clear-water flows and the second with bed load transport, and both tests were run under uniform flow condition. Uniform gravels of d_{50} = 4 mm were glued uniformly on the flume bottom with cement slurry to create a fixed bed. Longitudinal bed-slopes, S = 0.5% was maintained. A constant water discharge of 0.075 m^3/s was fed into the channel with uniform flow depth of 0.102 m in the working section and stable water surface. Feeding of gravels into the flow was made with a hopper located at the upstream of the flume. The bed load transport rate was 4.44×10^{-2} Kg/m.s computed by Meyer-Peter [45] formula. The non-cohesive gravel transport occurred as bed-load without any bed form development, maintaining a dynamic equilibrium condition. The shear-particle Reynolds numbers was found more than 70 and represented a rough-turbulent flow conditions. Other experimental details are given in Table 1.

Table 1. Experimental data: h = flow depth, U = mean velocity, F = flow Froude number, u_{*_s} = shear velocity measured from slope, u_{*_τ} = shear velocity measured from RSS, R_* = particle shear Reynolds number, g_b = bed-load transport rate

d_{50} = 4 mm, S = 0.5 %	Clear Water	Bed load
h (m)	0.102	0.102
U (m/s)	0.81	0.81
F	0.8	0.8
u_{*_s} (m/s)	0.07	0.07
u_{*_τ} (m/s)	0.067	0.060
R_*	204	183
g_b (kg/sm)	-	4.4×10^{-2}

A 5 cm down looking *Vectrino*$^+$ probe was used to measure the stream wise velocity fluctuations. The sampling rate was fixed at 100 Hz with an acoustic frequency of 10 MHz. At each point data were recorded for 300 seconds to obtain time-independent averaged velocity and turbulence characteristics. The measuring point was located at a distance of 6 m from the flume inlet. In this paper the bed surface along the centerline of the flume considered as x-axis and positive in the stream wise direction. For this experimental study the data filtration was performed by the *acceleration thresholding method* [Goring and Nikora, 2002]. The filtration process performed in two steps: 1) Firstly, a threshold values (= 1 to 1.5) for despiking were chosen to fit the data plots with the Kolmogorov "–5/3 scaling-law" in the inertial frequency range by trial and error. [Lacey and Roy, 2008]. Instantaneous streamwise velocity fluctuations (u') and the velocity power spectra produced no discrete spectral peak for $f > 0.5$ Hz, and the signals for $f \le 0.5$ Hz and $f > 0.5$ Hz contained large-scale motions and pure turbulence, respectively; 2) therefore, a high-pass filter with a cut-off frequency of 0.5 Hz was used for despiking the contaminated data. Fig. 2b shows the velocity power spectrum of filtered data and at frequencies from 0.5 to 20 Hz the data plots are well in conformity with the expected -5/3 slope

IV. RESULTS AND DISCUSSIONS

A. *Mobile Bed And Spectral Sub-Regimes*

Initially, we approached with an expectation that the spectral sub ranges in the velocity power spectra for bed load transport will address similar results as those found in the fixed bed. Interestingly, a close observation of the spectral signals in the production sub regime for bed load transport depicted shifting of frequency range. In case of fixed bed experiment under clear water flows, it is only the bed roughness that influences near bed turbulent flow characteristics. However, in mobile bed flows, the transport of bed particles introduced additional variability in the velocity field resulting the shifting of production regime towards high frequency level and produced discrete fluctuations at the production sub range. The velocity power spectrum of the streamwise velocity signals are plotted at two different locations along the vertical line in both clear water and bed load cases. The locations are leveled as 1.25 and 5 mm above the bed surface, respectively. The velocity power spectrum obtained from filtered streamwise velocity signals at the first location (z/h = 0.0122) depicted two clear scaling ranges. For relatively high frequencies (f = 0.5 Hz to 20 Hz), the slope of the velocity power spectra in the inertial sub range is −5/3 under clear water flows. A second scaling range is observed between $f >$ 0.07 Hz and < 0.5, for which the slope of velocity power spectra is −1 which refer to turbulent production range (Fig. 4a). The velocity power spectrum at the same location in presence of bed load reveals a shifting of turbulent production range (low-frequency regime) toward the higher frequencies at f = 0.15 Hz to 1.5 Hz with a spectral slope −1 (Fig. 4b).

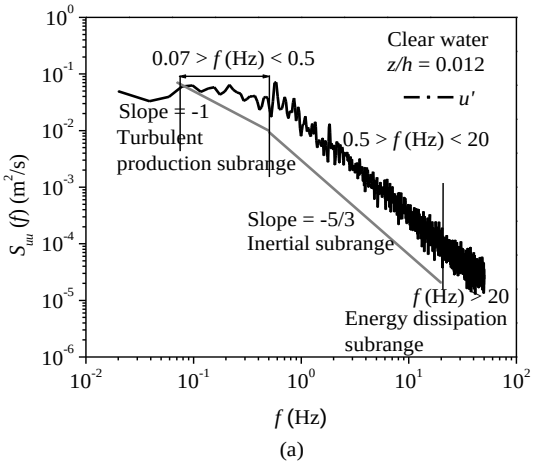

(a)

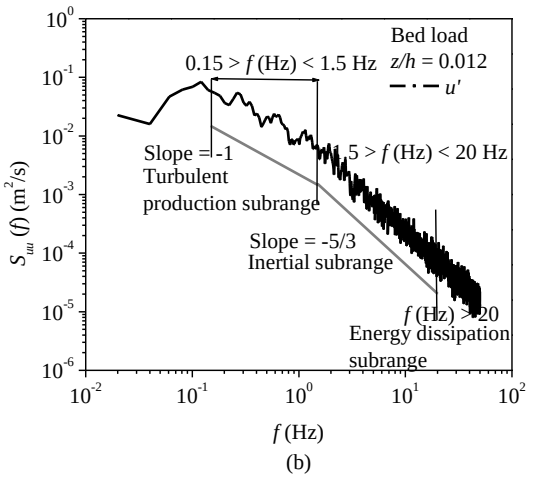

(b)

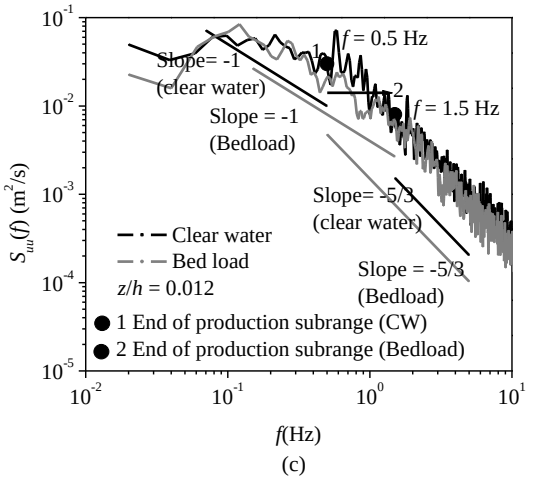

(c)

Fig. 4 Velocity power spectra S_{uu}(f) (a) clear-water conditions (b) bed-load and (c) shifting of production sub range at z/h = 0.012

The starting point of production regime observed at 0.07 Hz and extended up to 1.5 Hz in comparison to its clear water counterpart (0.5 Hz) and explained in Fig.4c. We interpret this shifting of subrange as a mark of additional variability in the velocity field on account of transport of bed particles. As we moved away the bed, the shifting of the turbulent production regime gradually reduces which attributed the decays in influence of bed load transport on turbulent production subrange. At second location (z/*h* = 0.05), the low frequency regime were within *f* = 0.07 Hz to 0.5 Hz and *f* = 0.1 Hz to 1 Hz for clear water and bed load transport, respectively as demonstrated in Fig.5 (a, b). This indicate similar production sub ranges at two vertical points under clear water flow conditions but the shifting narrowed down at second location in comparison to former location for bed load transport (Fig 5b). From the above observations it can be interpreted that the bed load transport influence significantly the velocity power spectrum in the range of *f* < 0.5 Hz. Now, next to turbulent production range, the inertial sub range of velocity power spectra both for clear water and bed load transport are satisfactorily characterized by the Kolmogorov -5/3 scaling-law. The data plots of filtered velocity power spectrum are used to detrmine average value of $S_{uu}k_w(k_w^{5/3})$ in order to obtain TKE dissipation rate ε and illustrated in later section.

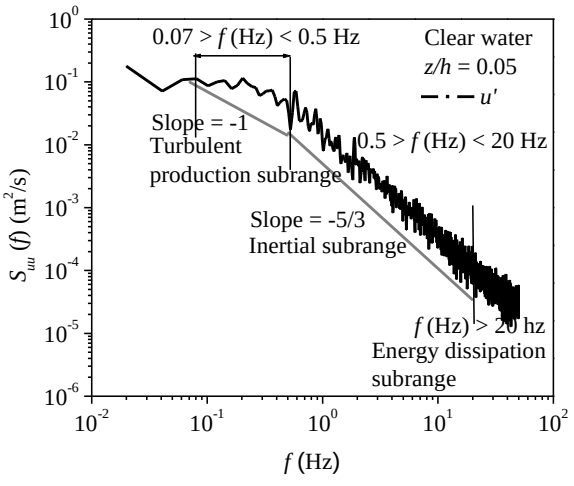

(a)

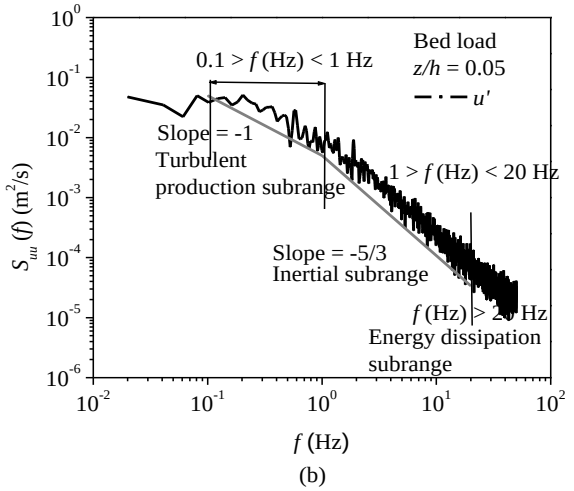

(b)

Fig. 5 Velocity power spectra $S_{uu}(f)$ (a) without bed-load and (b) bed-load at z = 5 mm,

B. *Turbulent Length Scale And Eddy Sizes In Mobile Bed Flows*

The velocity fluctuations and TKE-dissipation rate are associated to turbulent length scale and eddy sizes. Exchange of momentum and energy in the flows are mainly account for the largest length scale eddies. The physical boundary of the flows has an important role on eddy sizes. The size of the smallest scale of the flows is determined by the viscosity. For a statistically steady turbulent flow, the dissipation of turbulent energy associated to the small scale eddies counterbalance the turbulent energy associated to large scale eddies. Taylor micro scale represents the eddy size with corresponding length scale of turbulence and given by

$$\zeta_T = \left(\frac{15\upsilon\sigma_u^2}{\varepsilon}\right)^{0.5} \quad (5)$$

where $\sigma_u = (\overline{u'u'})^{0.5}$ = turbulence intensity in stream wise directions and ε = turbulent kinetic energy dissipation rate. Fig. 6a presents the variation of the normalized Taylor microscale $\hat{\zeta}_T = d_{50}/\zeta_T$, versus z/h. Near the bed ($z \le 0.1h$), $\hat{\zeta}_T$ is smaller in mobile bed flows in comparison to clear-water conditions. In the main flow region ($z > 0.1h$), the values of $\hat{\zeta}_T$ is almost same and decreases away from the bed. The near-bed values of ζ_T are 0.7 and 1.5 mm in case of without bed load and bed, respectively, showing that the eddy size next to the bed increases in bed load case. Furthermore, to address the TKE dissipation rate another length scale of the Kolmogorov microscale, ζ_K is applied and expressed as

$$\zeta_K = \left[\frac{\upsilon^3}{\varepsilon}\right]^{\frac{1}{4}} \quad (6)$$

where υ = kinematic viscosity of the fluid. The normalized Kolmogorov microscale $\hat{\zeta}_K = d_{50}/\zeta_K$ is plotted with z/h as shown in Fig. 6b. Similar to earlier length scale, near the bed ($z \le 0.1h$), $\hat{\zeta}_K$ is smaller in case of bed load than without bed load conditions. In the main flow region ($z > 0.1h$), the vertical profile of $\hat{\zeta}_K$ are narrowed down and diminishes away from the bed.

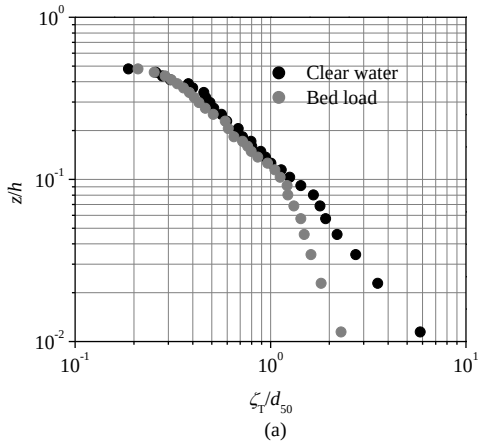

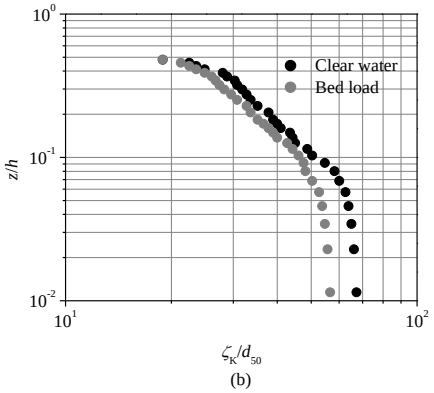

Fig. 6 Ratio of sediment size to the (a) Taylor microscale, ζ_T and (b) the Kolmogorov microscale, ζ_K for clear-water and mobile bed conditions

C. *Turbulent Kinetic Energy Budget*

All the turbulent kinetic energy budget components in Eq. (4) are made nondimensional by multiplying h/u_*^3 and represented as T_P, T_D, P_D and E_D. In order to obtain TKE-dissipation rate, the data plots of $S_{uu}k_w(k_w^{5/3})$ and k_w represents an average value of $S_{uu}k_w(k_w^{5/3})$ which is approximately constant as demonstrated in Fig. 7 (a, b). It represents a sub range of k_w. The energy dissipation rate ε is then obtained from Eq. (3) given as $\varepsilon = [0.5(S_{uu}(k_w) \times k_w^{1.66}]^{1.5}$, where, k_w = radian wave number in streamwise direction, $S_{uu}(k_w)$ = spectral density or wavenumber spectrum for u'. The average value of ε in near-bed region for mobile bed Test Runs are significantly found lesser with respect to clear water conditions (Fig. 7 a,b). At $z/h = 0.012$, the mean value of ε in clear water conditions is found to be higher than mobile bed conditions and revealed a notable change in TKE-dissipation rate in mobile bed. However, this differences in TKE-dissipation rate is narrowed down in the main flow region away the bed and the average value of ε is measured at $z/h = 0.05$ and 0.10 for both the flow conditions and described in Fig. 7(a,b).

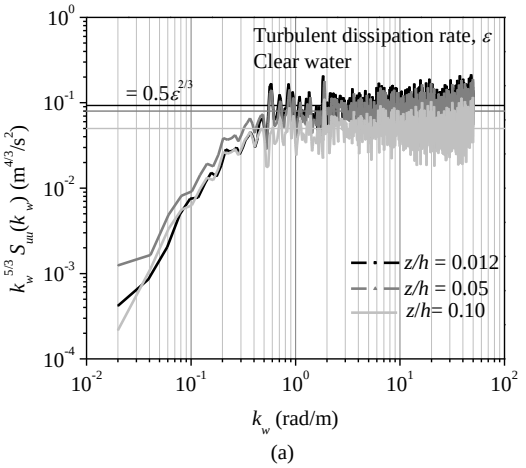

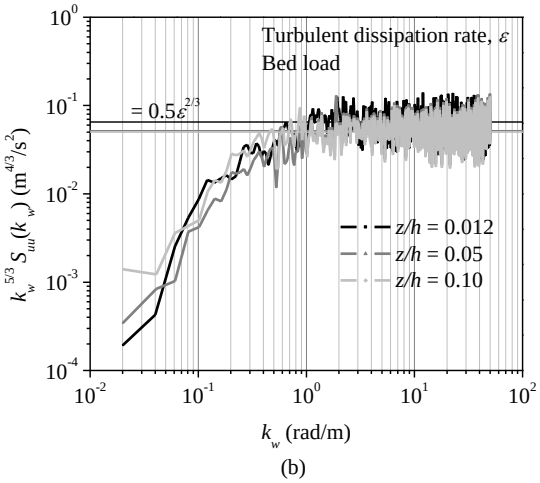

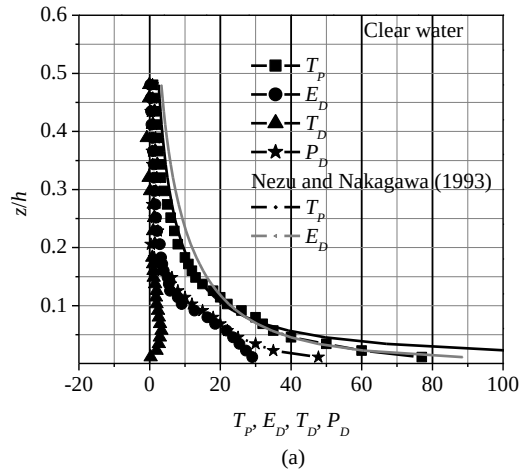

Fig. 7 Average energy dissipation rate, ε for (a) without bed load and (b) bed load conditions at z/h = 0.012, 0.5, and 0.10

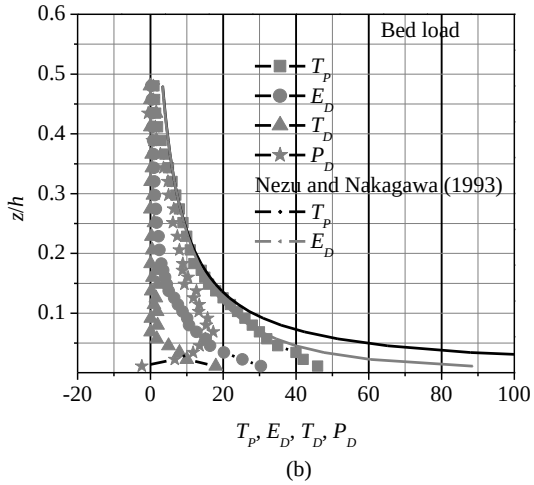

Fig. 8 TKE-budgets components for (a) clear-water and (b) mobile bed conditions

Figures 8(a, b) show the variations of T_P, T_D, P_D and E_D with z/h for the clear water and mobile bed conditions, respectively. T_P in the near bed region shows larger amplification and gradually reduces in the main flow region. For $z/h < 0.1$, the value of T_P for clear water flow is greater than that for the bedload transport, and for $z/h \geq 0.1$, the value of T_P are almost equal in both the cases. The data plots reveals that the bed roughness under clear water in the near bed flow zone ($z/h < 0.1$) resulted a larger value of T_P for the clear water conditions in comparison to mobile bed flows. The vertical distributions of E_D with z/h are presented in Fig. 8(a, b). The E_D reaches their maximum value near the bed and importantly, the E_D for the fixed bed conditions is found to be larger than that for the mobile bed and the reason behind this is attributed to the larger value of $\bar{u}$ for clear water conditions than that for bed load transport. The T_D for both the flow condition shows higher magnitude in the near bed region. In mobile bed flows, the T_D value is higher than those of its counterpart clear water conditions. The difference in the magnitude of T_D obtained for the clear water and bedload transport conditions is caused by the difference in temporal velocity fluctuations induced by the two beds. Fig. 8 (a, b) also depicts the variations of P_D with z/h for the mobile bed and clear water flow conditions. The data plots reveals that in mobile bed flows the P_D begin with negative values and attains maximum magnitude at z/h = 0.05. However, the P_D value gradually reduces with an increase in z/h. The data plots in Fig. 8 (a, b) describe the influence of bed load transport on pressure energy diffusion rate and the negative value (P_D = –2.5) attribute an increase of turbulence production in the near-bed flow region. The profile of T_P and E_D distributions are well in agreement with Nezu and Nakagawa [24] but shows some differences in magnitude and this is on account of experimental conditions. The bed-load influence is also apparent in the T_P and E_D distributions. The bed load transport reduces T_P significantly and E_D weakly and this occurs due to the enhanced damping of near-bed turbulent shear stress which is well in conformity with Dey et al. [15].

V. CONCLUSIONS

Respond of noncohesieve bed-load sediment transport on velocity power spectra of Acoustic-Doppler velocimetry data have been studied experimentally and compared with those in clear-water flows. A 5 cm down looking *Vectrino*$^+$ was used to capture velocity fluctuations over a mobile-bed. Influence of bed load transport on spectral density, turbulent length scale, TKE-dissipation rate and energy budget have been analyzed. Analysis of experimental data revealed some significant differences in the turbulent flow characteristics under both clear-water and mobile bed flow conditions and these are summarized below:

1) The velocity power spectra shows two distinct frequency ranges. An inertial sub range with a slope of −5/3 is observed at high frequencies. At lower frequencies, another scaling range with spectral slope of approximately −1 is found. In bed load transport, the turbulence production sub range shows a shifting of frequency range toward the higher frequency range.

Shifting of frequency range implies the influence of bed load transport on velocity power spectra.

2) The bed roughness significantly influence the size of eddies. Both the turbulent length scale in the order of Taylor microscale and Kolmogorov scale reveal an amplification of eddy sizes next to the bed in mobile bed flow conditions. In the outer-layer ($z > 0.1h$), no significant differences in eddy size were noticed and decreased away from the channel bed.
3) Results of TKE budget revealed that the influence of bed-load transport reduces the turbulent production rate and the pressure energy diffusion becomes negative implying a gain in turbulence production.

REFERENCES

1. Wiberg, P. L., Smith, J. D., "Velocity distribution and bed roughness in high-gradient streams", *Water Resour. Res*., (1991), 27(5), 825–838.
2. Dinehart, R. L., "Evolution of coarse gravel bed forms: Field measurements at flood stage", *Water Resour. Res.*, (1992), 28(10), 2667–2689.
3. Robert, A., Roy, A. G., De Serres, B., "Changes in velocity profiles at roughness transitions in coarse-grained channels", *Sedimentology*, (1992), 39: 725–735.
4. Buffin-Bélanger, T., Roy, A. G., "Effects of a pebble cluster on the turbulent structure of a depth-limited flow in a gravel-bed river", *Geomorphology* (1998), 25: 249–267, doi:10.1016/S0169-555X(98)00062-2.
5. Lacey, R. W. J., Roy, A. G., "A comparative study of the turbulent flow field with and without a pebble cluster in a gravel bed river", *Water Resour. Res*., (2007), 43, W05502, doi:10.1029/2006WR005027.
6. Hardy, R. J., Best, J. L., Lane, S. N., Carbonneau, P. E., "Coherent flow structures in a depth-limited flow over a gravel surface: The role of near-bed turbulence and influence of Reynolds number", *J. Geophys. Res*., (2009), 114, F01003, doi:10.1029/2007JF000970.
7. Nikora, V. I., Goring, D. G., Biggs, B. J. F., "On gravel-bed roughness characterization", *Water Resour. Res*., (1998): 34(3), 517–527.
8. Voulgaris, G., Trowbridge, J. H., "Evaluation of the acoustic Doppler velocimeter ADV for turbulence measurements", *J. Atmos. Ocean. Technol*, (1998) 15(1), 272–289.
9. Goring, D. G., Nikora, V. I., "Despiking acoustic Doppler velocimeter data", *J. Hydraul. Eng*., (2002): 128(1), 117–126.
10. Lane, et al. "Three-dimensional measurement of river channel flow processes using acoustic Doppler velocimetry", *Earth Surf. Processes Landforms*, (1998), 23, 1247–1267.
11. Wahl, T.L., "Analyzing ADV data using WinADV", *Proc., 2000 Joint Conf. on Water Resources Engineering and Water Resources Planning & Management*, ASCE, (2000).
12. García, C. M., Cantero, M.I., Niño, Y., García, M. H., "Turbulence measurements with acoustic Doppler velocimeters", *J. Hydraul. Eng*., (2005), 131(12): 1062–1073.
13. Cea, L., Puertas, J., Pena, L., "Velocity measurements on highly turbulent free surface flow using ADV", *Exp. Fluids*, (2007), 42: 333–348.
14. Dey, S., Das, R., "Gravel-bed hydrodynamics: Double-averaging approach", *J. Hydraul. Eng.* (2012), 138(8), 707-725, DOI: 10.1061/(ASCE)HY.1943-7900.0000554.
15. Dey et al., "Turbulence in mobile-bed streams", Acta Geophysica,(2012), 60(6), pp 1547–1588
16. Lien, R. C., D'Asaro, E. A., "Measurement of turbulent kinetic energy dissipation rate with a Lagrangian float", *J. Atmos. Oceanic Tech*. (2006), 23: 964–976, doi:10.1175/ JTECH1890.1
17. Bluteau, C. E., Jones, N. L., Ivey, G. N., "Estimating turbulent kinetic energy dissipation using the inertial subrange method in environmental flows", Limnol. Oceanogr. Meth. (2011), 9: 302–321. doi:10.4319/lom.2011.9.302.
18. Singh, A., Porte-Agel, F., Foufoula- Georgiou, F. E., "On the influence of gravel bed dynamics on velocity power spectra", *Water Resour Res*., (2010) 46:W04509.
19. Perry. A.E., Henbest, S. M., Chong, M.S., "A theoretical and experimental study of wall turbulence", *J. Fluid Mech*. (1986), 165, pp. 163-199.
20. Katul, G.G., Chu, C. R., Parlange, M. B., Albertson, J. D., Ortenburger, T. A., "Low wavenumber spectral characteristics of velocity and temperature in the atmospheric boundary layer", *J. Geophys. Res*., (1995), 100, 14, 243–14, 255.
21. Porté-Agel, F., Meneveau, C., Parlange, M. B., "A scale-dependent dynamic model for large-eddy simulation: Application to a neutral atmospheric boundary layer", *J. Fluid Mech*., (2000), 415, 216–284.
22. Kader, B. A., Yaglom, A. M., "Spectra and correlation functions of surface layer atmospheric turbulence in unstable thermal stratification in Turbulence and Coherent Structures", (1991), edited by O. Métais, M. Lesieur, pp. 387–412, Kluwer Acad., Dordrecht, Netherlands.
23. Kolmogorov, A., "Dissipation of energy in the locally isotropic turbulence, in Turbulence: Classic Papers on Statistical Theory", (1961), edited by S. K. Friedlander and L. Topper, pp. 151–155, Wiley Intersci., N. J.Hoboken.
24. Nezu, I., Nakagawa, H., *Turbulence in Open-Channel Flows*, Balkema, Rotterdam (1993).
25. Nikora, V.I., Goring, D.G., "Flow turbulence over fixed and weakly mobile gravel beds". *J Hydraul. Eng*., (2000), 126(9):679–690.
26. Nikora, V., "Hydrodynamics of gravel-bed rivers: Scale issues, in Gravel-Bed Rivers VI: From Process Understanding to River Restoration", edited by H. Habersack, H. Piegay, and M. Rinaldi, pp. 61–81, *Elsevier*, (2008), New York.
27. Owen, P. R., "Saltation of uniform grains in air", *J. of Fluid Mech.*, (1964), Vol. 20, pp. 225–242.
28. Smith, J. D., McLean, S. R., "Spatially averaged flow over a wavy surface", *J. of Geophy. Res.: Oceans*, (1977), Vol. 82, No. 12, pp. 1735–1746.
29. Gyr, A., Schmid, A., "Turbulent flows over smooth erodible sand beds in flumes", *J. of Hydraul. Res*., (1997), Vol. 35, No. 4, pp. 525–544.
30. Drake, T. G., Shreve Dietrich, W. E., Whiting, P. J., Leopold, L. B., "Bed load transport of fine gravel observed by motion picture photography", *J. of Fluid Mech*.,(1988), Vol. 192, pp. 193–217.
31. Kirkbride, A. D., "Observations of the influence of bed roughness on turbulence structure in depth-limited flows over gravel beds, in Turbulence: Perspectives on Flow and Sediment Transport", (1993), edited by N. J. Clifford, J. R. French, J. Hardisty, pp. 185–196, *John Wiley*, Chichester, U. K.
32. Kirkbride, A. D., McLelland, M. J., "Visualization of the turbulent flow structures in a gravel bed river", *Earth Surf. Processes Landforms*, (1994), 19, 819–825.
33. Kirkbride, A. D., Ferguson, R. I., "Turbulent flow structure in a gravel-bed river: Markov chain analysis of the fluctuating velocity profile", *Earth Surf. Processes Landforms*, (1995), 20, 721–733.
34. Lamarre, H., Roy, A. G., "Reach scale variability of turbulent flow characteristics in a gravel-bed river", *Geomorpholgy*, (2005), 60, 95–113.
35. Shvidchenko, A. B., Pender, G., "Macro-turbulent structure of open-channel flow over gravel beds", *Water Resour. Res*., (2001), 37(3), 709–719.
36. Roy, A. G., Buffin-Belanger, T., Lamarre, H., Kirkbride, A. D., "Size, shape and dynamics of large-scale turbulent flow structures in a gravel-bed river", *J. Fluid Mech*., (2004), 500, 1–27.
37. Lacey, R. W. J., Roy, A. G., "Fine-scale characterization of the turbulent shear layer of an in stream pebble cluster", *J. of Hydraul. Eng.*, (2008), Vol. 134, No. 7, pp. 925–936.
38. Best, J. L., "On the interactions between turbulent flow structure, sediment transport and bed form development: Some considerations from recent experimental research, in Turbulence: Perspectives on Flow and Sediment Transport", (1993), edited by N. J. Clifford, J. R. French, J. Hardisty, pp. 61–92, *John Wiley*, Chichester, U. K.
39. Robert, A., Roy, A. G., De Serres, B., "Spacetime correlations of velocity measurements at a roughness transition in a gravel-bed river, in Turbulence: Perspectives on Flow and Sediment Transport", (1993), edited by N. J. Clifford, J. R. French, J. Hardisty, pp. 167–183, *John Wiley*, Chichester, U. K.
40. Schmeeckle, M. W., Nelson, J. M., Shreve, R. L., "Forces on stationary particles in near-bed turbulent flows", *J. Geophys. Res*., (2007), 112, F02003, doi:10.1029/2006JF000536.
41. Hardy, R. J., Best, J. L., Lane, S. N., Carbonneau, P. E., "Coherent flow structures in a depth-limited flow over a gravel surface: The role of near-bed turbulence and influence of Reynolds number", *J. Geophys. Res*., (2009), 114, F01003, doi:10.1029/2007JF000970.
42. Robinson, S. K., "The kinematics of turbulent boundary layer structure". NASA, (1991), TM 103859.
43. Pope, S.B., *Turbulent flows*. Cambridge University Press, Cambridge (2001)

44. Monin, A.S., Yaglom, A.M., "Statistical fluid mechanics, volume II: mechanics of turbulence", Dover Publications, New York (2007).
45. 45. Meyer-Peter, E., "Transport des matières solides en general et problèmes speciaux", *Bulletin Genie Civil d'Hydraul,* (1951), *Fluviale*, Tome V.

AUTHORS PROFILE

Dr. Ratul Das obtained Ph.D from IIT Kharagpur in Water Resources Engineering. His area of research is Fluvial Hydraulics. He has significant contributions in the field of Fluvial Hydraulics and published his research works in many reputed journals. Presently he is associate Professor in National Institute of Technology Agartala.